ARTICLE
Journal of Cellular Biochemistry 112:723–733 (2011)

Journal of Cellular Biochemistry

Positive Regulation of Inositol 1,4,5-Trisphosphate-Induced Ca^{2+} Release by Mammalian Target of Rapamycin (mTOR) in RINm5F Cells

Marc-Olivier Frégeau, Yannik Régimbald-Dumas, and Gaétan Guillemette*

Faculty of Medicine and Health Sciences, Department of Pharmacology, Université de Sherbrooke, Sherbrooke, Quebec, Canada J1H 5N4

ABSTRACT

The inositol 1,4,5-trisphosphate receptor (IP_3R), a ligand-gated Ca^{2+} channel, is the main regulator of intracellular Ca^{2+} mobilization in non-excitable cells. An emerging body of evidence suggests that specific regulatory control of the Ca^{2+} signaling pathway is modulated by the activation of additional signaling pathways. In the present study, we investigated the influence of the PI3-kinase/mammalian target of rapamycin (mTOR) pathway on the activity of the IP_3R/Ca^{2+} signaling pathway in RINm5F cells. We used a co-immunoprecipitation approach to show that mTOR physically interacts with IP_3R-3 in an mTOR activity-dependent manner. We also showed that IP_3R is phosphorylated by mTOR in cellulo. All the conditions known to modulate mTOR activity (IGF-1, wortmannin, rapamycin, PP242, and nutrient starvation) were shown to modify carbachol-induced Ca^{2+} signaling in RINm5F cells. Lastly, we used an assay that directly measures the activity of IP_3R, to show that mTOR increases the apparent affinity of IP_3R. Given that mTOR controls cell proliferation and cell homeostasis, and that Ca^{2+} plays a key role in these two phenomena, it follows that mTOR facilitates IP_3R-mediated Ca^{2+} release when the nutritional status of cells requires it. J. Cell. Biochem. 112: 723–733, 2011. © 2010 Wiley-Liss, Inc.

KEY WORDS: INOSITOL 1,4,5-TRISPHOSPHATE RECEPTOR; mTOR; PHOSPHORYLATION; CA2+

Ca^{2+} is a key second messenger that influences a vast array of cellular processes, including contraction, secretion, cell growth, and cell proliferation. In non-excitable cells, intracellular Ca^{2+} signaling is induced by a wide variety of hormones and growth factors that activate phospholipase C isoforms that hydrolyze phosphatidylinositol 4,5-bisphosphate to generate the second messenger inositol 1,4,5-trisphosphate (IP_3). IP_3 activates a receptor/channel (IP_3R) on the endoplasmic reticulum and releases stored Ca^{2+} that diffuses throughout the cytosol and triggers Ca^{2+}-dependent cellular responses [Berridge, 1993; Joseph and Ryan, 1993; Yoshida and Imai, 1997]. In mammalian cells, three IP_3R subtypes have been identified. Most cell types express different proportions of each subtype [Furuichi et al., 1993; Maranto, 1994; Wojcikiewicz and He, 1995; Perez et al., 1997; Holtzclaw et al., 2002]. IP_3R subtypes are highly homologous and have an analogous general structure, including an N-terminal ligand-binding domain, a C-terminal channel domain, and an intervening regulatory domain containing binding sites for Ca^{2+}, nucleotides, calmodulin, diverse proteins, and modulatory factors, as well as putative phosphorylation sites for several protein kinases [Foskett et al., 2007]. The regulatory domain shares the least homology among the three IP_3R subtypes. This relatively poor homology likely confers specific pharmacological and functional properties on each IP_3R subtype.

Specific regulatory control of the Ca^{2+} signaling pathway occurs by the concomitant activation of other signaling pathways. For example, the cAMP-PKA pathway potentiates Ca^{2+} signaling by increasing the sensitivity of IP_3R-1, IP_3R-2, and IP_3R-3 [DeSouza et al., 2002; Tang et al., 2003; Soulsby et al., 2004; Tu et al., 2004; Wagner et al., 2004; Arguin et al., 2007; Regimbald-Dumas et al., 2007]. Numerous isolated observations suggest that the PI3K-Akt pathway may also influence the Ca^{2+} signaling pathway. In neuronal and endocrine cells, IP_3R is a direct substrate for Akt kinase [Khan et al., 2006; Koulen et al., 2008]. In hippocampal neurons, progesterone potentiates Ca^{2+} release by IP_3R via an Akt-mediated mechanism [Hwang et al., 2009]. In pancreatic islet cells, insulin potentiates G_q protein-coupled receptor activation of phospholipase C and Ca^{2+} signaling through an mammalian target of rapamycin

Grant sponsor: Canadian Institutes of Health Research.

*Correspondence to: Prof. Gaétan Guillemette, Faculty of Medicine and Health Sciences, Department of Pharmacology, Université de Sherbrooke, 3001-12th Avenue North, Sherbrooke, QC, Canada J1H 5N4.
E-mail: gaetan.guillemette@usherbrooke.ca

Received 18 May 2010; Accepted 15 December 2010 • DOI 10.1002/jcb.23006 • © 2011 Wiley-Liss, Inc.
Published online 29 December 2010 in Wiley Online Library (wileyonlinelibrary.com).

(mTOR)-dependent pathway [Kisfalvi et al., 2007]. IP_3-induced Ca^{2+} release from cerebellar microsomes is decreased by the mTOR inhibitor rapamycin [Dargan et al., 2002]. In voltage-clamped colonic myocytes, rapamycin also decreases the Ca^{2+} response evoked by IP_3R activation [MacMillan et al., 2005]. In line with these observations, our recent work showed that Hsp90 decreases IP_3R activity in an insulin-dependent manner [Nguyen et al., 2009]. Insulin modulates the interaction between Hsp90 and IP_3R via an unknown pathway involving Src and mTOR [Nguyen et al., 2009]. Based on this information, we hypothesized that mTOR may directly phosphorylate IP_3R and potentiate its activity.

mTOR is a Ser/Thr kinase that forms functional complexes with several protein partners including raptor and rictor. mTOR is activated mainly through the PI3K-Akt pathway [Hay and Sonenberg, 2004; Sancak et al., 2007] but also by amino acids through a pathway involving bidirectional transport of amino acids across the plasma membrane [Nicklin et al., 2009] and by Rag GTPase [Kim et al., 2008; Sancak et al., 2008]. Conversely, when the intracellular concentration of ATP is low, mTOR activity is suppressed through a pathway involving AMPK [Shaw, 2009]. As a central controller of cell growth, mTOR plays a key role in development and aging, and has been implicated in disorders such as cancer [Shaw and Cantley, 2006; Dann et al., 2007], cardiovascular disease [Wang et al., 2009], obesity [Dann et al., 2007; Rui, 2007; Mori et al., 2009a], and diabetes [Dann et al., 2007; Leibowitz et al., 2008; Mori et al., 2009b].

mTOR is also involved in the control of cell proliferation, motility, and survival, as well as gene transcription, protein synthesis, and in the spatial control of cell growth by regulating the actin cytoskeleton [Fingar and Blenis, 2004; Jacinto et al., 2004; Sarbassov et al., 2004; Tsang et al., 2007]. Because many of these processes are Ca^{2+}-dependent, it is coherent that mTOR could modulate the Ca^{2+} signaling system via direct control over IP_3R activity.

The purpose of the present study was therefore to investigate the regulation of IP_3R activity by mTOR. Since no investigation on the susceptibility of the different IP_3R subtypes to mTOR regulation has been published to date, we conducted the present study using rat insulinoma RINm5F cells that predominantly (95%) express the IP_3R-3 isoform. We showed that, in RINm5F cells, IP_3R-3 interacted with, and was efficiently phosphorylated by mTOR. We also showed that the inhibition of mTOR decreased CCh-induced Ca^{2+} responses and IP_3-induced Ca^{2+} release. These results suggest that mTOR positively regulates IP_3R-3-mediated Ca^{2+} release in RINm5F cells.

MATERIALS AND METHODS

RPMI medium, fetal bovine serum (FBS), and penicillin–streptomycin–glutamine were purchased from Gibco Life Technologies (Gaithersburg, MD). Phosphate-free DMEM was purchased from Wisent (St-Bruno, QC, Canada). $[^{32}P]P_i$ (orthophosphate), 0.2 μm nitrocellulose membranes, Western Lightning™ Chemiluminescence Reagent Plus, Kodak BioMax MR films, and BioMax Light films were purchased from Perkin Elmer (Boston, MA). Mouse anti-IP_3R-3 antibody, which recognizes an N-terminal epitope of the protein was purchased from BD Biosciences (Mississauga, ON, Canada). Protein AG-agarose was purchased from Santa Cruz Technology (Santa Cruz, CA). Peroxidase-conjugated donkey anti-rabbit-IgG and sheep anti-mouse-IgG were bought from General Electric Healthcare (Baie d'Urfe, QC, Canada). ATP, IGF-1, bovine serum albumin (BSA), PP242, creatine phosphokinase, phosphocreatine, saponin, thapsigargin, L-leucine, wortmannin, and ionomycin were purchased from Sigma–Aldrich (Oakville, ON, Canada). Rabbit anti-mTOR antibody was purchased from Cell Signaling Technology (Boston, MA). Carbachol (CCh), fura-2 (free acid), fura-2/AM, β-glycerophosphate, rabbit anti-raptor antibody were purchased from Calbiochem (San Diego, CA). Rabbit anti-rictor antibody was purchased from Bethyl Laboratories (Burlington, ON, Canada). Polyvinylidene fluoride (PVDF) membranes (0.2 μm) were purchased from Millipore Corporation (Billerica, MA). Complete protease inhibitor cocktail was purchased from Roche Molecular Biochemicals (Laval, QC, Canada). Sodium pyrophosphate and sodium fluoride were purchased from Fisher Scientific (Ottawa, ON, Canada). Rapamycin (mTOR inhibitor) was purchased from USBiological (Swampscott, MA).

CELL CULTURES

RINm5F cells (American Type Culture Collection, Manassas, VA) were cultured at 37°C in a humidified 5% CO_2 atmosphere in RPMI medium containing L-glutamine (2 mM), FBS (10%, v/v), penicillin (100 U/ml), and streptomycin (100 μg/ml). The cells were passaged every 3–4 days and were used when they reached 75% confluence.

Immunoprecipitation and Western blots. RINm5F cells (10^7 cells) were washed twice with phosphate-buffered saline (PBS, 137 mM NaCl, 3.5 mM KCl, 17.4 mM Na_2HPO_4, 3.5 mM NaH_2PO_4, 0.9 mM $CaCl_2$, 0.9 mM $MgCl_2$) and solubilized in lysis buffer (1% Triton X-100, 150 mM NaCl, 50 mM Tris–HCl, pH 7.4) supplemented with 10 mM NaF, 2 mM $Na_4P_2O_7$, 2 mM β-glycerophosphate, and 1× complete protease inhibitor cocktail for 60 min at 0°C. Insoluble material was precipitated by centrifugation at 13,000*g* for 15 min at 4°C. For the immunoprecipitation studies, identical amounts of protein from each cell extract were incubated overnight at 4°C with anti-IP_3R-3, anti-mTOR, anti-raptor, or anti-rictor antibody, and 50 μl of protein-A/G-agarose beads. Non-specifically bound proteins were removed by washing the beads three times with ice-cold lysis buffer. Bound material was resuspended in 50 μl of 1× Laemmli buffer and boiled for 5 min. Cell lysates or immunoprecipitated proteins were resolved by SDS–PAGE (6% resolving gel) at a constant voltage of 130 V for 150 min. The protein bands were then electrotransferred to a 0.2 μm nitrocellulose membrane for 90 min at 4°C at a constant voltage of 100 V in transfer buffer (96 mM glycine, 10 mM Tris-base, 0.01% SDS, 20% methanol, pH 8.5). The blots were blocked for 1 h at room temperature in TBS-T buffer (20 mM Tris-base, 150 mM NaCl, 0.1% Tween-20, 5% BSA, pH 7.5) and incubated overnight at 4°C with mouse anti-IP_3R-3 (1:1,000), rabbit anti-mTOR (1:500), rabbit anti-raptor (1:500), or rabbit anti-rictor (1:500) antibody in TBS-T. After three washes with TBS-T, the blots were incubated with peroxidase-conjugated sheep anti-mouse-IgG (1:20,000) or donkey

anti-rabbit-IgG (1:20,000) antibody for 1 h at room temperature in TBS-T. After three washes with TBS-T, the immune complexes were visualized using Western Lightning™ Chemiluminescence Reagent Plus.

In cellulo phosphorylation of IP_3R-3. RINm5F cells (10^7 cells) were washed twice with HBSS (20 mM Hepes, pH 7.4, 120 mM NaCl, 5.3 mM KCl, 0.8 mM $MgSO_4$, 1.8 mM $CaCl_2$) and incubated with phosphate-free DMEM supplemented with L-glutamine (2 mM) and [^{32}P]P_i (50 μCi/ml) for 4 h at 37°C. The cells were stimulated for different time periods under different conditions, then washed and immediately solubilized in lysis buffer. After immunoprecipitation, SDS–PAGE, and electrotransfer to a PVDF membrane, labeled bands were revealed by autoradiography using BioMax ML films to detect the quantity of IP_3R-3. The PVDF membrane was washed in water for 12 h than the phosphorylated IP_3R-3 was revealed by autoradiography using BioMax MR films with an intensifying screen for 7 days at −80°C. The degree of phosphorylation was quantified by densitometric analysis using Image-J® software (developed by the NIH).

Dynamic videoimaging of cytosolic Ca^{2+}. RINm5F cells grown on glass coverslips were washed twice with HBSS buffer and incubated with 0.15 μM fura-2/AM in HBSS buffer for 20 min at room temperature in the dark. After a de-esterification step (incubation in fresh HBSS for 20 min at room temperature), the coverslips were inserted into a circular open-bottom chamber and mounted on the stage of a Zeiss Axiovert microscope fitted with an Attofluor Digital Imaging and Photometry System (Attofluor Inc., Rockville, MD). This system allows simultaneous data acquisition from up to 99 user-defined variably sized regions of interest (or cells) per field of view. It can also calculate, at any time point, the average response of all the cells selected in the field. Fluorescence from isolated fura 2-loaded cells was monitored by videomicroscopy using alternative excitatory wavelengths of 334 and 380 nm, with an emitted fluorescence of 510 nm. All experiments were done at room temperature, and the data were expressed as the intracellular free Ca^{2+} concentration (nM) calculated from the 334/380 fluorescence ratio.

IP_3-induced Ca^{2+} release. RINm5F cells (3×10^7 cells) were permeabilized in 2 ml of cytosol-like buffer (20 mM Tris-HCl, pH 7.4, 10 mM NaCl, 110 mM KCl, 5 mM KH_2PO_4, 2 mM $MgCl_2$) supplemented with 150 μg/ml of saponin, 0.5 μM fura-2 acid, 20 U of creatine kinase, and 20 mM phosphocreatine. Fura-2 fluorescence

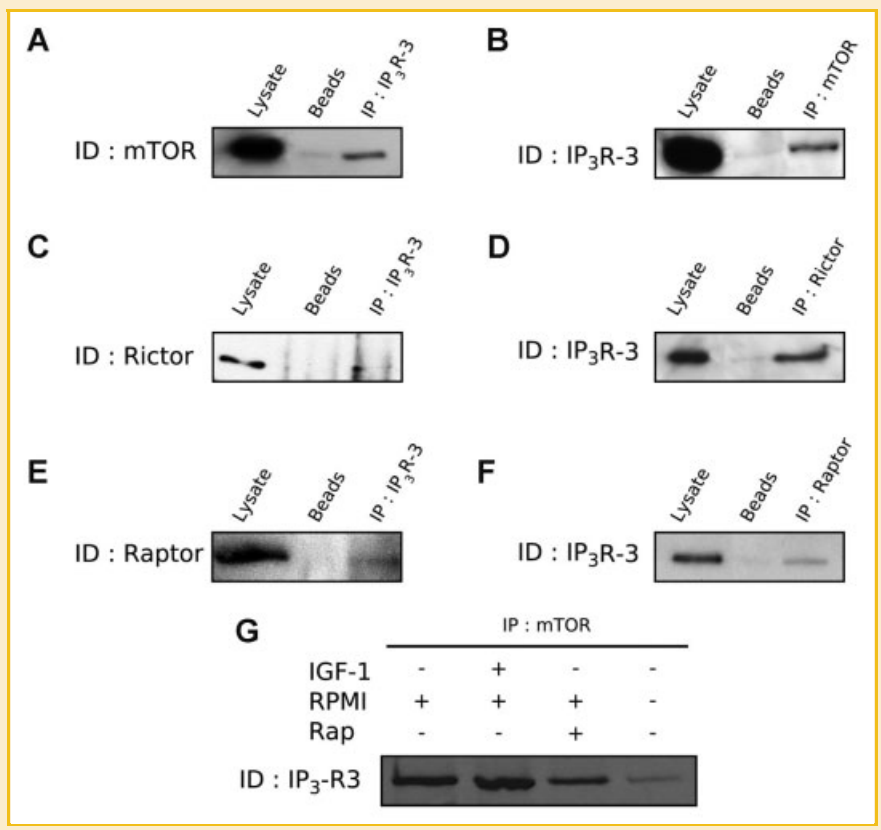

Fig. 1. mTOR interacts with IP_3R-3 in RINm5F cells. Panels A, C, and E: After solubilizing RINm5F cells in lysis buffer, the proteins were immunoprecipitated with anti-IP_3R-3 antibody, separated by 6% SDS–PAGE, and immunodetected with anti-mTOR (A), anti-rictor (C), or anti-raptor (E) antibody. Panels B, D, and F: The solubilized proteins were immunoprecipitated with anti-mTOR antibody (B), anti-rictor antibody (D), or anti-raptor antibody (F), and separated by a 6% SDS–PAGE. IP_3R-3 was then immunodetected with anti-IP_3R-3 antibody. Panel G: RINm5F cells were starved of nutrient (or not) for 4 h. They were then treated with IGF-1, rapamycin (rap), or vehicle for 10 min, solubilized in lysis buffer, immunoprecipitated with anti-mTOR antibody, and immunodetected with anti-IP_3R-3 antibody. These results are representative of three independent experiments.

was monitored at 37°C with a Hitachi F-2000 spectrofluorometer (Hitachi Scientific Instruments Inc., Hialeah, FL) with alternative excitation wavelengths of 340 and 380 nm, with an emission wavelength of 510 nm. The amount of Ca^{2+} released by IP_3 was calculated based on the fluorescent signal obtained with an exogenously added Ca^{2+} standard (4 nmol $CaCl_2$). The maximal fluorescence (R_{max}) and minimal fluorescence (R_{min}) ratios were determined by adding 2 mM Ca^{2+} then 10 mM EGTA to the cell suspension. When needed, the free Ca^{2+} concentration was calculated according to Grynkiewicz et al. [1985].

DATA ANALYSIS

All experiments were performed at least three times. Results are presented as means ± standard deviations (SD). When needed, the data were analyzed using Student's *t*-test. Results were considered statistically significant when $P < 0.05$ (*).

RESULTS

mTOR CO-IMMUNPRECIPITATES WITH IP_3R-3 IN RINm5F CELL EXTRACTS

To verify whether IP_3R interacts with mTOR in growing cells, we used an anti-IP_3R-3 antibody to immunoprecipitate the IP_3R-3 subtype that is predominantly expressed (95%) in RINm5F cells [Wojcikiewicz and He, 1995]. The Western blot shown in Figure 1A indicates that mTOR was abundantly expressed in RINm5F cells. When cell extracts were immunoprecipitated with an anti-IP_3R-3 antibody, mTOR was detected in the immunoprecipitate. In the absence of the anti-IP_3R-3 antibody, mTOR did not adhere to the agarose beads. To further confirm the presence of a physical interaction between mTOR and IP_3R-3, cell extracts were immunoprecipitated with an anti-mTOR antibody. Figure 1B shows that IP_3R-3 was expressed in RINm5F cells and that it co-immunoprecipitated with mTOR. We next verified whether raptor and rictor (the common partners of mTOR) also co-immunoprecipitated with IP_3R-3. Figure 1C shows that when cell extracts were immunoprecipitated with an anti-IP_3R-3 antibody, rictor was detected in the immunoprecipitate. The reciprocal co-immunoprecipitation shown in Figure 1D further suggests that rictor interacts with the IP_3R-3. Similarly, Figure 1E shows that when the cell extracts were immunoprecipitated with an anti-IP_3R-3 antibody, raptor was detected in the immunoprecipitate. The reciprocal co-immunoprecipitation shown in Figure 1F further suggests that raptor interacts with the IP_3R-3. Negative controls using an anti-hemaglutinin IgG confirmed that the co-immunoprecipitations of IP_3R-3, raptor and rictor were not due to non-specific interaction with irrelevant IgG or with the agarose beads (data not shown). These results suggest that IP_3R-3 physically interacts with the mTOR signaling complexes. We then verified whether the interaction between mTOR and IP_3R-3 was modified under conditions known to increase (stimulating cells with IGF-1) or decrease (pre-treatment with rapamycin or 4 h nutrient starvation) the activity of mTOR. When the cell extracts were immunoprecipitated with the anti-mTOR antibody, the co-immunoprecipitation of IP_3R-3 was decreased by rapamycin and by a 4 h nutrient starvation period, but was increased when the intact cells were stimulated with IGF-1 (Fig. 1E). These results suggest that the in cellulo interaction between mTOR and IP_3R-3 was dependent on the level of activity of mTOR.

mTOR PHOSPHORYLATES IP_3R-3

mTOR is a kinase that regulates the activity of its target substrates by phosphorylation. Since its association with IP_3R-3 is dependent on its level of activity, it is very likely that mTOR phosphorylates IP_3R-3. To verify this hypothesis, we evaluated the impact of different conditions known to affect the activity of mTOR on the phosphorylation level of IP_3R-3 in intact cells. Figure 2A shows that under basal conditions (RPMI+) IP_3R-3 was already phosphorylated in intact RINm5F cells. A pre-treatment of the cells with IGF-1 increased the level of phosphorylation of IP_3R-3 whereas a pre-treatment of the cells with rapamycin decreased the level of phosphorylation of IP_3R-3. The densitometric analysis of the autoradiograms (Fig. 2B) indicated that IGF-1 increased the level of phosphorylation of IP_3R-3 to 192% (compared to control cells) whereas rapamycin decreased the level of phosphorylation of IP_3R-3 to 63%. These results suggested that endogenous mTOR phosphorylated IP_3R-3 in intact RINm5F cells.

PI3K AND mTOR MODULATE CCh-INDUCED CA^{2+} RELEASE IN RINm5F CELLS

To determine the functional consequence of IP_3R-3 phosphorylation by mTOR, we evaluated the cytosolic Ca^{2+} concentration in intact

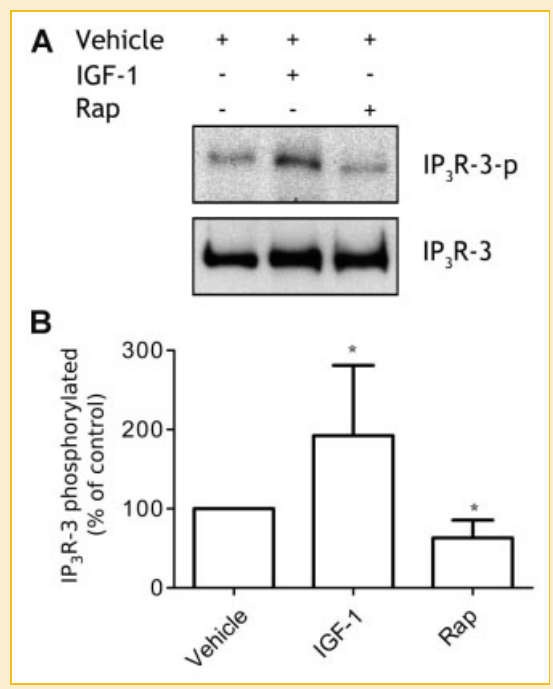

Fig. 2. mTOR phosphorylates IP_3R-3. Panel A: In cellulo phosphorylation of IP_3R-3. RINm5F cells were labeled for 4 h with 75 μCi/mL [^{32}P]P_i and then incubated for 15 min with rapamycin (rap) or IGF-1. After lysing the cells, the proteins were immunoprecipitated with anti-IP_3R-3 antibody, resolved by 6% SDS–PAGE, and revealed by autoradiography (IP_3R-3-p) or Western blotting (IP_3R-3). Panel B: Densitometric analysis of the autoradiograms shown in panel B (means ± SD of data from eight independent experiments, *$P < 0.05$ compared to the control).

RINm5F cells bathed in a nominally Ca^{2+}-free medium. Under these conditions, the agonist-induced intracellular Ca^{2+} increase was exclusively due to Ca^{2+} release from the endoplasmic reticulum through IP_3R. Figure 3A shows that under basal conditions (vehicle) a low dose of the Ca^{2+}-mobilizing agonist carbachol (CCh, 3 μM) produced a transient Ca^{2+} increase with peak amplitude of 44.2 ± 4.5 nM Ca^{2+}. After a pre-treatment with 0.4 μM wortmannin (a PI3K inhibitor), CCh produced a significantly lower Ca^{2+} response, with a peak amplitude of 25.6 ± 6.6 nM Ca^{2+}. IGF-1 is a known activator of the PI3K pathway. Figure 3C,D show that the Ca^{2+} response induced by 3 μM CCh was significantly increased in cells pre-treated with 100 ng/ml IGF-1 (peak amplitude of 75.0 ± 9.2 nM Ca^{2+}) compared to control cells (peak amplitude of 53.5 ± 5.1 nM Ca^{2+}). Clearly PI3K, an upstream activator of mTOR, can regulate IP_3-induced Ca^{2+} release in RINm5F cells.

To directly assess the impact of mTOR on IP_3-induced Ca^{2+} release activity, we repeated the experiment using rapamycin, a well-characterized mTOR inhibitor. Figure 4A,B show that the Ca^{2+} response induced by CCh (3 μM) was significantly lower in cells pre-treated with rapamycin (peak amplitude of 35.3 ± 7.2 nM Ca^{2+}) than in control cells (peak amplitude of 64.9 ± 11.7 nM Ca^{2+}). The dose–response curve for CCh-induced Ca^{2+} release in rapamycin-treated cells (Fig. 4C) showed a rightward shift (EC_{50} of 14.5 ± 4.6 μM CCh) compared to that obtained with control cells (EC_{50} of 6.8 ± 1.9 μM CCh). Figure 4D shows the dose-dependent inhibitory effect of rapamycin on CCh-induced Ca^{2+} release activity. In paired experiments (similar to those shown in Fig. 4A,B), there was no significant difference in the amount of Ca^{2+} released by untreated and rapamycin-treated cells at a maximal concentration of 300 μM CCh (as also seen in Fig. 4C). A treatment with 2 μM thapsigargin (SERCA pump inhibitor), followed by the addition of 1.8 mM extracellular $CaCl_2$, revealed that the IP_3-releasable Ca^{2+} pool (61.7 ± 8.5 and 59.6 ± 8.2 nM Ca^{2+}) and the store-operated Ca^{2+} entry pathway (94.3 ± 4.6 and 99.8 ± 3.1 nM Ca^{2+}) were similar in control and rapamycin-treated cells, respectively (Fig. 4E,F). These results suggest that mTOR potentiated IP_3-induced Ca^{2+} release by increasing the apparent affinity of IP_3R-3. They also show that mTOR did not affect the content of the intracellular pool of Ca^{2+} nor the function of the capacitative Ca^{2+} entry channel, two important components of the Ca^{2+} signaling machinery.

To further confirm that mTOR potentiated IP_3-induced Ca^{2+} release activity, we tested the effect of different mTOR modulators. PP242 is known to inhibit mTOR by targeting its ATP-binding domain. Figure 5A,B show that the Ca^{2+} response induced by 3 μM CCh was significantly decreased in cells pre-treated with 10 μM PP242 (peak amplitude of 25.73 ± 2.2 nM Ca^{2+}) compared to that of control cells (peak amplitude of 38.03 ± 4.7 nM Ca^{2+}). In addition, mTOR is inhibited by low nutrient levels and growth factor deprivation, but is activated by amino acids, particularly branched

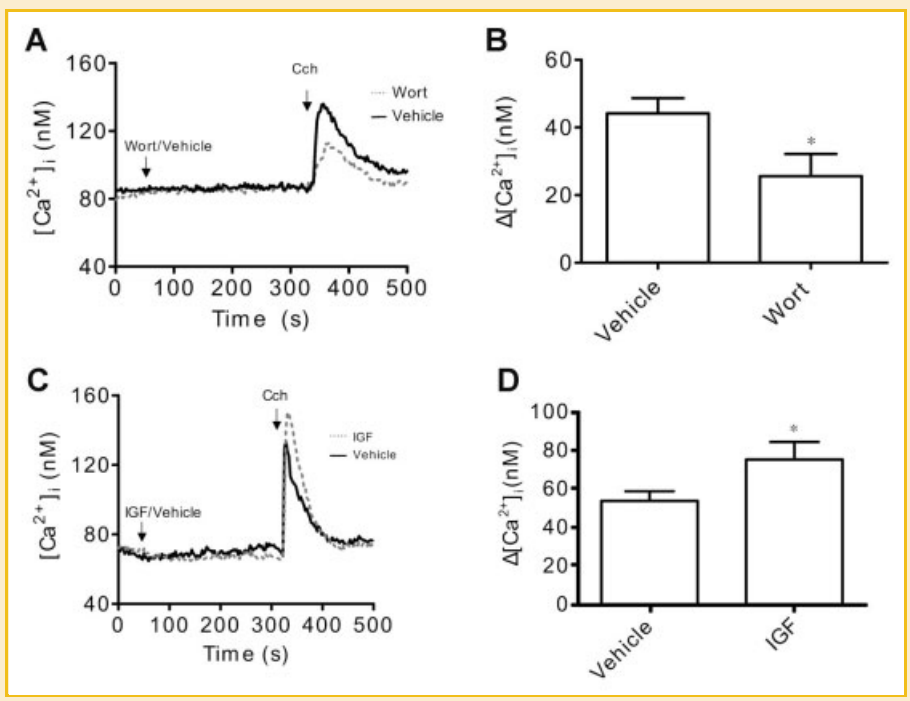

Fig. 3. The PI3K pathway modulates CCh-induced Ca^{2+} release in intact RINm5F cells. RINm5F cells were loaded with Fura-2/AM and bathed in a nominally Ca^{2+}-free extracellular medium. The cells were imaged using a Zeiss Axiovert microscope (40× oil immersion objective) coupled to an Attofluor imaging system. Panel A: Representative recordings of intracellular Ca^{2+} levels before and after the addition of 3 μM CCh to cells pre-treated with vehicle or with wortmannin (Wort). Each trace shows the average response of 60–75 cells per microscope field. Panel B: Average Ca^{2+} responses (peak amplitude) of cells stimulated with 3 μM CCh after a pre-treatment with vehicle or with wortmannin (mean ± SD of results obtained from three independent experiments, $^*P < 0.05$ compared to control). Panel C: Representative recordings of intracellular Ca^{2+} levels before and after the addition of 3 μM CCh to cells pre-treated with vehicle or with IGF-1 (IGF). Panel D: Average Ca^{2+} responses (peak amplitude) of cells stimulated with 3 μM CCh after a pre-treatment with vehicle or with IGF-1 (mean ± SD of results obtained from three independent experiments, $^*P < 0.05$ compared to control).

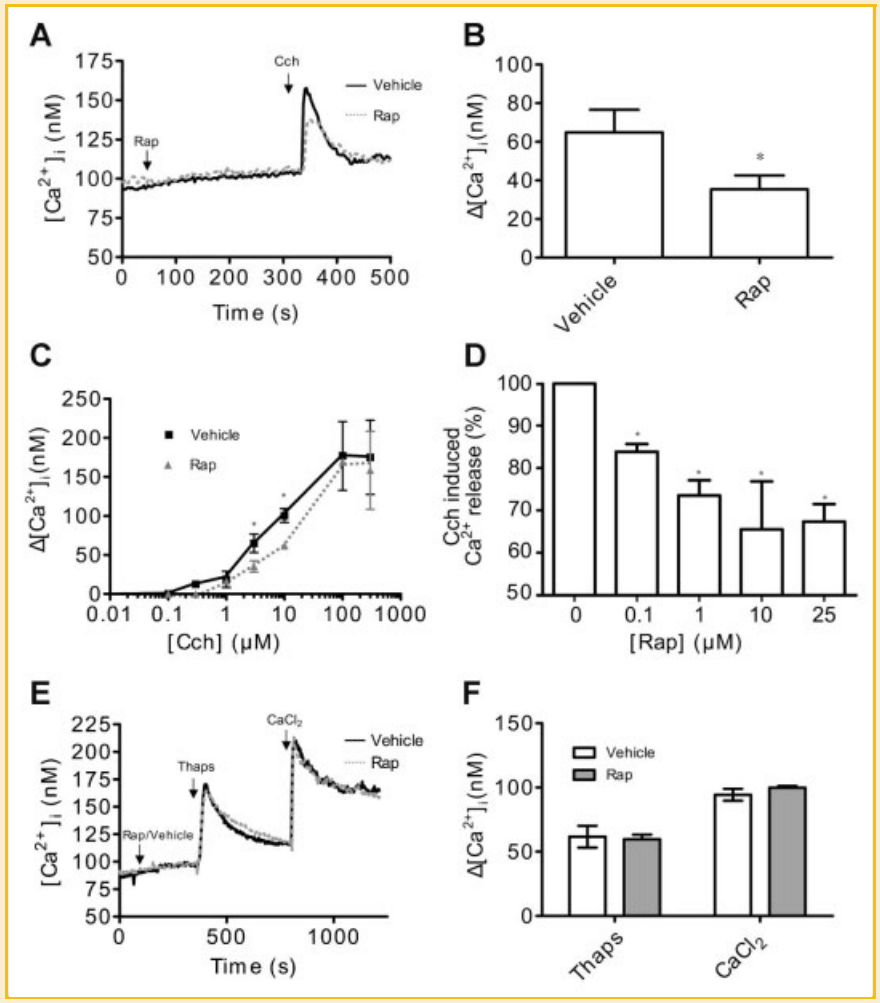

Fig. 4. Rapamycin decreases CCh-induced Ca^{2+} release in intact RINm5F cells. RINm5F cells were loaded with Fura-2/AM and bathed in a nominally Ca^{2+}-free extracellular medium. The cells were imaged using a Zeiss Axiovert microscope (40× oil immersion objective) coupled to an Attofluor imaging system. Panel A: Representative recordings of intracellular Ca^{2+} levels before and after the addition of 3 μM CCh to cells pre-treated with vehicle or rapamycin (rap). Panel B: Average Ca^{2+} responses (peak amplitude) of cells stimulated with 3 μM CCh after a pre-treatment with vehicle or rapamycin (mean ± SD of results obtained from three independent experiments, $^{*}P < 0.05$ compared to control). Panel C: Dose–response curves for CCh-induced Ca^{2+} release in intact RINm5F cells pre-treated with rapamycin (triangle) or vehicle (square). Panel D: Dose-dependent inhibitory effect of rapamycin on 3 μM CCh-induced Ca^{2+} release in intact RINm5F cells. After a pre-treatment with increasing concentrations of rapamycin, RINm5F cells were stimulated with 3 μM CCh and their intracellular Ca^{2+} level was measured by Fura-2 fluorescence as described in Panel A. Results are expressed as % of the response obtained in the absence of rapamycin (100%). These results (mean ± SD) are representative of three independent experiments, $^{*}P < 0.05$ compared to control). Panel E: Store-operated Ca^{2+} entry in RINm5F cells pre-treated with vehicle or with rapamycin. Representative recordings of intracellular Ca^{2+} levels obtained after the depletion of the intracellular Ca^{2+} store with thapsigargin (Thaps) and after restoring the extracellular Ca^{2+} concentration to 1.8 mM. Panel F: Average Ca^{2+} responses (peak amplitude) obtained after treating the cells with thapsigargin and after restoring the extracellular Ca^{2+} concentration (means ± SD of results obtained from five independent experiments, $^{*}P < 0.05$ compared to control).

amino acids such as L-leucine [Nicklin et al., 2009]. Figure 6 shows that the Ca^{2+} response induced by CCh (3 μM) was significantly lower in cells that had been starved of nutrient and growth factor for 4 h (peak amplitude of 44.7 ± 8.1 nM Ca^{2+}) than in control cells (peak amplitude of 60.3 ± 7.9 nM Ca^{2+}). After a 4 h period of nutrient starvation, cells that had been treated with 10 mM L-leucine produced a CCh-induced Ca^{2+} response similar to that of control cells (peak amplitude of 62.8 ± 12.9 nM of Ca^{2+}). Interestingly, rapamycin abolished the effect of L-leucine on starved cells (peak amplitude of 37.3 ± 10.6 nM Ca^{2+}). These results suggest that mTOR potentiated IP_3-induced Ca^{2+} release in RINm5F cells (Fig. 6).

PRE-TREATMENT OF RINm5F CELLS WITH RAPAMYCIN DECREASES IP_3-INDUCED CA^{2+} RELEASE

To directly evaluate the effect of mTOR on IP_3R activity, we used a direct IP_3-induced Ca^{2+} release assay that measures the ambient Ca^{2+} concentration by fura-2 fluorescence. The assay directly measures the Ca^{2+} released via IP_3R in permeabilized cells when exogenous IP_3 is added. Figure 7A shows a typical experiment where 0.3 μM IP_3 released Ca^{2+} from permeabilized RINm5F cells. The amount of Ca^{2+} released was calibrated by the exogenous addition of 10 nmol $CaCl_2$. Figure 7A–C show that 0.3 μM IP_3 released less Ca^{2+} from permeabilized cells that had been pre-treated with

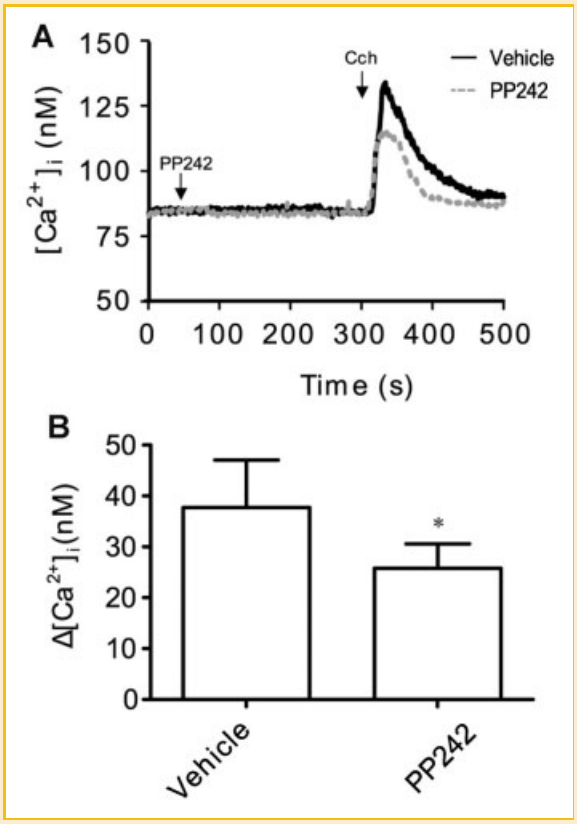

Fig. 5. PP242 decreases CCh-induced Ca^{2+} release in intact RINm5F cells. RINm5F cells were loaded with Fura-2/AM and bathed in a nominally Ca^{2+}-free extracellular medium. The cells were imaged using a Zeiss Axiovert microscope (40× oil immersion objective) coupled to an Attofluor imaging system. Panel A: Representative recordings of intracellular Ca^{2+} levels before and after the addition of 3 μM CCh to cells pre-treaded or not with 10 μM PP242.). Panel B: Average Ca^{2+} responses (peak amplitude) of cells stimulated with 3 μM CCh after a pre-treatment with vehicle or with PP242 (mean ± SD of results obtained from three independent experiments, $^*P < 0.05$ compared to control).

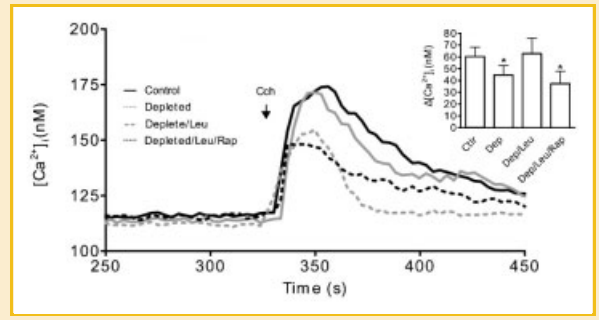

Fig. 6. Cellular nutritional status modulates CCh-induced Ca^{2+} release in intact RINm5F cells. RINm5F cells were loaded with Fura-2/AM and bathed in a nominally Ca^{2+}-free extracellular medium. The cells were imaged using a Zeiss Axiovert microscope (40× oil immersion objective) coupled to an Attofluor imaging system. Panel A: Representative recordings of intracellular Ca^{2+} levels before and after the addition of 3 μM CCh to cells deprived of nutrients (or not) and pre-treated (or not) with L-leucine (Leu) or with rapamycin. The inset shows the average Ca^{2+} responses (peak amplitude) of cells stimulated with 3 μM CCh after a pre-treatment with vehicle, rapamycin or L-leucine (mean ± SD of results obtained from three independent experiments, $^*P < 0.05$ compared to control).

rapamycin (peak amplitude of 280.5 ± 67.0 nM Ca^{2+}) than from control permeabilized cells (peak amplitude of 609.2 ± 81.8 nM Ca^{2+}). Figure 7D shows that the dose–response curve for IP_3-induced Ca^{2+} release from rapamycin-treated cells was shifted to the right (EC_{50} of 0.61 ± 0.05 μM IP_3) compared to the curve obtained with control cells (EC_{50} of 0.29 ± 0.06 μM IP_3). In paired experiments (similar to those shown in Fig. 7A,B), there was no significant difference in the amount of Ca^{2+} released by control and rapamycin-treated cells at a maximal dose of 10 μM IP_3 (also seen in Fig. 7D). A treatment with 2 μM ionomycin revealed that the IP_3-releasable Ca^{2+} pool of rapamycin-treated cells (2.12 ± 0.39 μM Ca^{2+}) was similar to that of control cells (2.01 ± 0.29 μM Ca^{2+}; Fig. 7E). These results suggest that mTOR potentiated agonist-induced Ca^{2+} responses in RINm5F cells by increasing the apparent affinity of IP_3R. Similarly, Figure 8A–C show that 0.3 μM IP_3 released less Ca^{2+} from permeabilized cells that had been pre-treated with 10 μM PP242 (peak amplitude of 226.2 ± 24.5 nM Ca^{2+}) than from control permeabilized cells (peak amplitude of 471.4 ± 43.5 nM Ca^{2+}). A treatment with 2 μM ionomycin revealed that the IP_3-releasable Ca^{2+} pool of PP242-treated cells (1.95 ± 0.19 μM Ca^{2+}) was similar to that of control cells (1.86 ± 0.28 μM Ca^{2+}; Fig. 8D).

DISCUSSION

In the present study, we used a co-immunoprecipitation approach to show that IP_3R-3 interacts physically with mTOR and with its common functional partners raptor and rictor. The interaction was strengthened under conditions that increased the activity of mTOR and was weakened under conditions that decreased the activity of mTOR. Similarly, we showed that the phosphorylation of IP_3R-3 was increased by IGF-1 and decreased by rapamycin. mTOR phosphorylates some of its substrates at a conserved non-catalytic residue within the motif Phe-X-X-Phe-Ser/Thr-Tyr (where X is any amino acid), which is conserved from yeast to mammals [Alessi et al., 2009]. Rat IP_3R-3 does not have such a motif. However, it was recently shown that mTOR can also target proline-directed sites [Brunn et al., 1997; Saitoh et al., 2002; Facchinetti et al., 2008; Ikenoue et al., 2008]. Rat IP_3R-3 has several Thr-Pro or Ser-Pro sites that could be targets for phosphorylation by mTOR. To our knowledge, we are the first to report a functional association between mTOR and IP_3R and to show that mTOR phosphorylates IP_3R-3. In a recent study showing that rapamycin decreases IP_3-induced Ca^{2+} release in colonic myocytes, MacMillan et al. [2005] could not co-immunoprecipitate mTOR with IP_3R-1. Either their cell model lacked an essential component or their experimental conditions did not favor a stable association between mTOR and IP_3R-1. Another likely explanation could be that the specificity of IP_3R subtypes may influence the stability of the complex with mTOR. While RINm5F cells are known to express almost exclusively IP_3R-3, the IP_3R subtypes expressed in colonic myocytes, and their relative proportions, are unknown. Further work is needed to verify these possibilities.

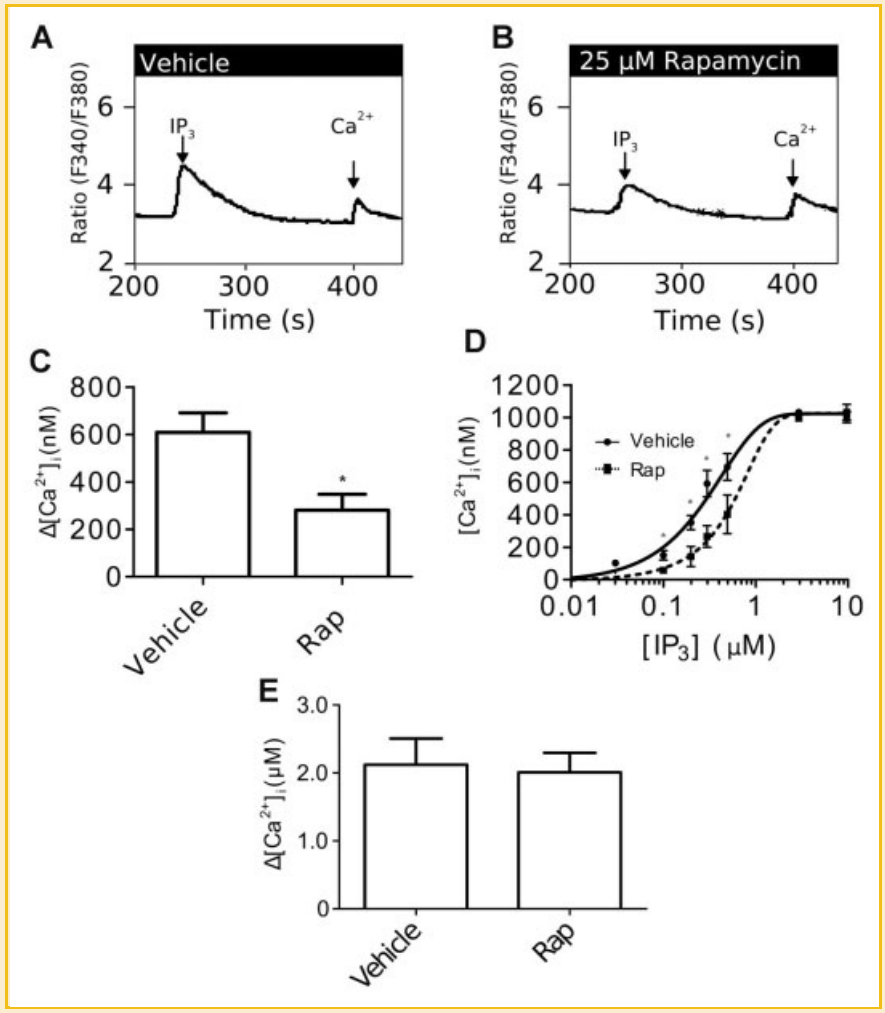

Fig. 7. Rapamycin decreases IP_3-induced Ca^{2+} release in permeabilized RINm5F cells. RINm5F cells (3×10^7) were permeabilized with 150 μg/ml saponin and pre-treated for 5 min with vehicle (A) or with rapamycin (B) in a cytosol-like medium containing 0.5 μM fura-2 acid. Ca^{2+} was then partially released with 0.3 μM IP_3. The amount of Ca^{2+} released by IP_3 was calibrated by adding 4 nmoles of exogenous Ca^{2+}. These traces are representative of results obtained in at least three independent experiments. Panel C: Average amounts of Ca^{2+} released from permeabilized cells stimulated with 0.3 μM IP_3 after a pre-treatment with vehicle or with rapamycin (mean ± SD of results obtained from three independent experiments, $^*P < 0.05$ compared to control). Panel D: Dose–response curves for IP_3-induced Ca^{2+} release from permeabilized cells pre-treated with vehicle (circle) or with rapamycin (square). Panel E: Total content of the intracellular Ca^{2+} store (released with 2 μM ionomycin) of permeabilized RINm5F cells pre-treated with vehicle (empty bar) or with rapamycin (filled bar). The data shown in panels D and E represent the means ± SD of results obtained from three independent experiments ($^*P < 0.05$ compared to control).

We used intact RINm5F cells bathed in a Ca^{2+}-free medium to show that wortmannin (PI3K inhibitor) decreases CCh-induced Ca^{2+} release, whereas IGF-1 increases CCh-induced Ca^{2+} release. These results are in agreement with several studies showing that Akt potentiates IP_3R-mediated Ca^{2+} release [Khan et al., 2006; Koulen et al., 2008; Hwang et al., 2009]. While these studies clearly identified Akt as an important component of the PI3K pathway involved in the regulation of IP_3R activity, they did not take into account the possible participation of mTOR, which is a downstream component of this pathway. We showed that rapamycin, PP242 and nutrient starvation decreased CCh-induced Ca^{2+} release, whereas L-leucine reversed the effect of nutrient starvation. These results clearly identified mTOR as a modulator of intracellular Ca^{2+} signaling. Because rapamycin did not modify the content of the thapsigargin-sensitive Ca^{2+} pool, the decreased Ca^{2+} release was likely due to a decrease in the activity of IP_3R. Dose–response curves for CCh-induced Ca^{2+} release were shifted rightward in the presence of rapamycin, indicating a decrease in the apparent affinity of IP_3R. To directly assess the effect of mTOR on IP_3R function, we investigated the effect of rapamycin and PP242 on IP_3-induced Ca^{2+} release in permeabilized RINm5F cells. This is a straightforward assay that evaluates the direct effect of IP_3 on its receptor/channel. As previously observed with intact cells, rapamycin did not modify the ionomycin-sensitive Ca^{2+} pool of permeabilized cells, indicating that mTOR acted on IP_3R. The rightward shift of the dose–response curve for IP_3-induced Ca^{2+} release also revealed that rapamycin decreases the apparent affinity of IP_3R in RINm5F cells.

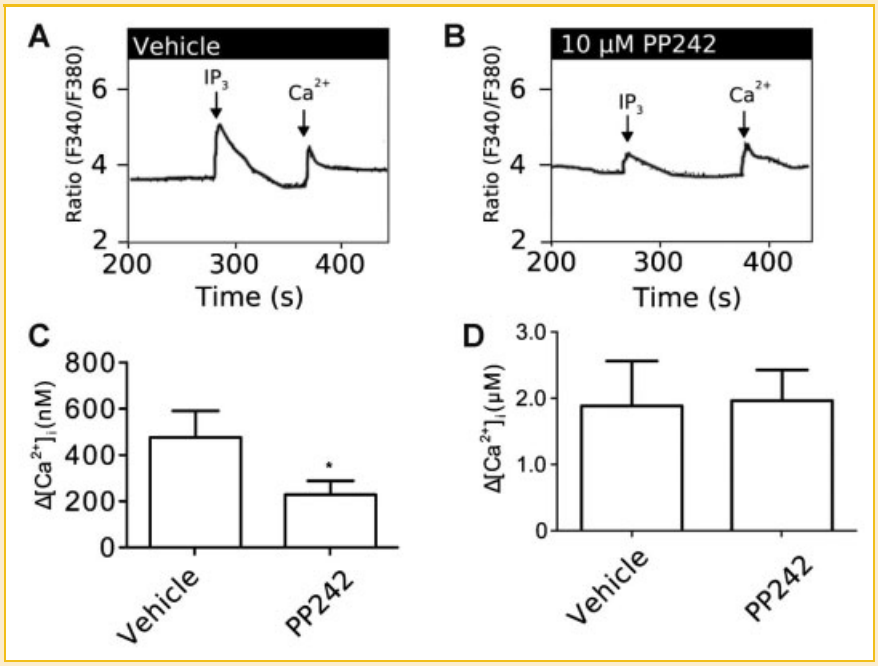

Fig. 8. PP242 decreases IP_3-induced Ca^{2+} release in permeabilized RINm5F cells. RINm5F cells (3×10^7) were permeabilized with 150 μg/ml saponin and pre-treated for 5 min with vehicle (A) or with 10 μM PP242 (B) in a cytosol-like medium containing 0.5 μM fura-2 acid. Ca^{2+} was then partially released with 0.3 μM IP_3. The amount of Ca^{2+} released by IP_3 was calibrated by adding 4 nmoles of exogenous Ca^{2+}. These traces are representative of results obtained in at least three independent experiments. Panel C: Average amounts of Ca^{2+} released from permeabilized cells stimulated with 0.3 μM IP_3 after a pre-treatment with vehicle or with PP242 (mean ± SD of results obtained from three independent experiments, $^*P < 0.05$ compared to control). Panel D: Total content of the intracellular Ca^{2+} store (released with 2 μM ionomycin) of permeabilized RINm5F cells pre-treated with vehicle (empty bar) or with PP242 (filled bar). The data shown in panels C and D represent the means ± SD of results obtained from three independent experiments ($^*P < 0.05$ compared to control).

In colonic myocytes, MacMillan et al. [2005] observed that rapamycin decreases IP_3-induced Ca^{2+} release, suggesting that mTOR plays a positive modulatory role via an unknown mechanism. Puzzlingly, they did not observe a similar effect of rapamycin in vascular myocytes. The authors suggested that this discrepancy may be due to differences in the two tissues. As mentioned above, the specific subtypes of IP_3R expressed in these tissues could explain, in part, such differences. To get a clear picture on the effect of mTOR on IP_3R, it is important to know which IP_3R subtypes are expressed in a particular cell type or, alternatively, to study tissues or cells that express only one subtype. We also observed that mTOR potentiated IP_3-induced Ca^{2+} release in AR4-2J cells that express almost exclusively the IP_3R-2 isoform [Regimbald-Dumas et al., 2011]. Therefore, mTOR appears to produce the same potentiating effect on IP_3R-2 and IP_3R-3 isoforms. Further work is needed to evaluate the effect of mTOR on IP_3R-1.

The fact that mTOR positively modulates IP_3R-3 activity in RINm5F cells indicates that mTOR is important in regulating Ca^{2+} signaling. Interestingly, Khan and Joseph [2010] recently showed that basal autophagic flux may be negatively regulated by IP_3R-dependent Ca^{2+} signals acting to maintain an elevated mTOR activity. They suggested that Ca^{2+} is a positive regulator of mTOR himself. IP_3R and mTOR seem to be intimately linked together, reciprocally regulating their activity. This cross-talk between the Ca^{2+} signaling and the PI3K/Akt/mTOR pathways associates two of the main pathways involved in cell growth and proliferation. Since the fine regulation of intracellular Ca^{2+} is involved in most cellular processes, it is coherent that mTOR, which is key for cell survival, regulates Ca^{2+} signaling. This regulatory role with respect to Ca^{2+} signaling provides further evidence for the involvement of mTOR in many disorders, including cancer, diabetes, obesity, and cardiovascular diseases.

In conclusion, we showed that in RINm5F cells mTOR phosphorylates IP_3R-3 and increases its sensitivity to IP_3, indicating that it is involved in the fine regulation of intracellular Ca^{2+} level and cell functions.

ACKNOWLEDGMENTS

This work is part of the PhD thesis of M.-O.F. It was supported by a grant from the Canadian Institutes of Health Research. M.-O.F. and Y.R.-D. hold studentship awards from the National Sciences and Engineering Research Council of Canada.

REFERENCES

Alessi DR, Pearce LR, Garcia-Martinez JM. 2009. New insights into mTOR signaling: mTORC2 and beyond. Sci Signal 2:pe27.

Arguin G, Regimbald-Dumas Y, Fregeau MO, Caron AZ, Guillemette G. 2007. Protein kinase C phosphorylates the inositol 1,4,5-trisphosphate receptor type 2 and decreases the mobilization of Ca^{2+} in pancreatoma AR4-2J cells. J Endocrinol 192:659–668.

Berridge MJ. 1993. Cell signalling. A tale of two messengers. Nature 365:388–389.

Brunn GJ, Fadden P, Haystead TA, Lawrence JC, Jr. 1997. The mammalian target of rapamycin phosphorylates sites having a (Ser/Thr)-Pro motif and is activated by antibodies to a region near its COOH terminus. J Biol Chem 272:32547–32550.

Dann SG, Selvaraj A, Thomas G. 2007. mTOR Complex1-S6K1 signaling: At the crossroads of obesity, diabetes and cancer. Trends Mol Med 13:252–259.

Dargan SL, Lea EJ, Dawson AP. 2002. Modulation of type-1 Ins(1,4,5)P3 receptor channels by the FK506-binding protein, FKBP12. Biochem J 361:401–407.

DeSouza N, Reiken S, Ondrias K, Yang YM, Matkovich S, Marks AR. 2002. Protein kinase A and two phosphatases are components of the inositol 1,4,5-trisphosphate receptor macromolecular signaling complex. J Biol Chem 277:39397–39400.

Facchinetti V, Ouyang W, Wei H, Soto N, Lazorchak A, Gould C, Lowry C, Newton AC, Mao Y, Miao RQ, Sessa WC, Qin J, Zhang P, Su B, Jacinto E. 2008. The mammalian target of rapamycin complex 2 controls folding and stability of Akt and protein kinase C. EMBO J 27:1932–1943.

Fingar DC, Blenis J. 2004. Target of rapamycin (TOR): An integrator of nutrient and growth factor signals and coordinator of cell growth and cell cycle progression. Oncogene 23:3151–3171.

Foskett JK, White C, Cheung KH, Mak DO. 2007. Inositol trisphosphate receptor Ca2+ release channels. Physiol Rev 87:593–658.

Furuichi T, Simon-Chazottes D, Fujino I, Yamada N, Hasegawa M, Miyawaki A, Yoshikawa S, Guenet JL, Mikoshiba K. 1993. Widespread expression of inositol 1,4,5-trisphosphate receptor type 1 gene (Insp3r1) in the mouse central nervous system. Receptors Channels 1:11–24.

Grynkiewicz G, Poenie M, Tsien RY. 1985. A new generation of Ca2+ indicators with greatly improved fluorescence properties. J Biol Chem 260:3440–3450.

Hay N, Sonenberg N. 2004. Upstream and downstream of mTOR. Genes Dev 18:1926–1945.

Holtzclaw LA, Pandhit S, Bare DJ, Mignery GA, Russell JT. 2002. Astrocytes in adult rat brain express type 2 inositol 1,4,5-trisphosphate receptors. Glia 39:69–84.

Hwang JY, Duncan RS, Madry C, Singh M, Koulen P. 2009. Progesterone potentiates calcium release through IP3 receptors by an Akt-mediated mechanism in hippocampal neurons. Cell Calcium 45:233–242.

Ikenoue T, Inoki K, Yang Q, Zhou X, Guan KL. 2008. Essential function of TORC2 in PKC and Akt turn motif phosphorylation, maturation and signalling. EMBO J 27:1919–1931.

Jacinto E, Loewith R, Schmidt A, Lin S, Ruegg MA, Hall A, Hall MN. 2004. Mammalian TOR complex 2 controls the actin cytoskeleton and is rapamycin insensitive. Nat Cell Biol 6:1122–1128.

Joseph SK, Ryan SV. 1993. Phosphorylation of the inositol trisphosphate receptor in isolated rat hepatocytes. J Biol Chem 268:23059–23065.

Khan MT, Joseph SK. 2010. The role of inositol trisphosphate receptors in autophagy in DT40 cells. J Biol Chem 285:16912–16920.

Khan MT, Wagner L II, Yule DI, Bhanumathy C, Joseph SK. 2006. Akt kinase phosphorylation of inositol 1,4,5-trisphosphate receptors. J Biol Chem 281:3731–3737.

Kim E, Goraksha-Hicks P, Li L, Neufeld TP, Guan KL. 2008. Regulation of TORC1 by Rag GTPases in nutrient response. Nat Cell Biol 10:935–945.

Kisfalvi K, Rey O, Young SH, Sinnett-Smith J, Rozengurt E. 2007. Insulin potentiates Ca^{2+} signaling and phosphatidylinositol 4,5-bisphosphate hydrolysis induced by Gq protein-coupled receptor agonists through an mTOR-dependent pathway. Endocrinology 148:3246–3257.

Koulen P, Madry C, Duncan RS, Hwang JY, Nixon E, McClung N, Gregg EV, Singh M. 2008. Progesterone potentiates IP(3)-mediated calcium signaling through Akt/PKB. Cell Physiol Biochem 21:161–172.

Leibowitz G, Cerasi E, Ketzinel-Gilad M. 2008. The role of mTOR in the adaptation and failure of beta-cells in type 2 diabetes. Diabetes Obes Metab 10(Suppl 4): 157–169.

MacMillan D, Currie S, Bradley KN, Muir TC, McCarron JG. 2005. In smooth muscle, FK506-binding protein modulates IP3 receptor-evoked Ca2+ release by mTOR and calcineurin. J Cell Sci 118:5443–5451.

Maranto AR. 1994. Primary structure, ligand binding, and localization of the human type 3 inositol 1,4,5-trisphosphate receptor expressed in intestinal epithelium. J Biol Chem 269:1222–1230.

Mori H, Inoki K, Munzberg H, Opland D, Faouzi M, Villanueva EC, Ikenoue T, Kwiatkowski D, MacDougald OA, Myers MG, Jr., Guan KL. 2009a. Critical role for hypothalamic mTOR activity in energy balance. Cell Metab 9:362–374.

Mori H, Inoki K, Masutani K, Wakabayashi Y, Komai K, Nakagawa R, Guan KL, Yoshimura A. 2009b. The mTOR pathway is highly activated in diabetic nephropathy and rapamycin has a strong therapeutic potential. Biochem Biophys Res Commun 384:471–475.

Nguyen N, Francoeur N, Chartrand V, Klarskov K, Guillemette G, Boulay G. 2009. Insulin promotes the association of heat shock protein 90 with the inositol 1,4,5-trisphosphate receptor to dampen its Ca^{2+} release activity. Endocrinology 150:2190–2196.

Nicklin P, Bergman P, Zhang B, Triantafellow E, Wang H, Nyfeler B, Yang H, Hild M, Kung C, Wilson C, Myer VE, MacKeigan JP, Porter JA, Wang YK, Cantley LC, Finan PM, Murphy LO. 2009. Bidirectional transport of amino acids regulates mTOR and autophagy. Cell 136:521–534.

Perez PJ, Ramos-Franco J, Fill M, Mignery GA. 1997. Identification and functional reconstitution of the type 2 inositol 1,4,5-trisphosphate receptor from ventricular cardiac myocytes. J Biol Chem 272:23961–23969.

Regimbald-Dumas Y, Arguin G, Fregeau MO, Guillemette G. 2007. cAMP-dependent protein kinase enhances inositol 1,4,5-trisphosphate-induced Ca^{2+} release in AR4-2J cells. J Cell Biochem 101:609–618.

Regimbald-Dumas Y, Fregeau MO, Guillemette G. 2011. Mammalian target of rapamycin (mTOR) phosphorylates inositol 1,4,5-trisphosphate receptor type 2 and increases its Ca(2+) release activity. Cell signal 23(1): 71–79.

Rui L. 2007. A link between protein translation and body weight. J Clin Invest 117:310–313.

Saitoh M, Pullen N, Brennan P, Cantrell D, Dennis PB, Thomas G. 2002. Regulation of an activated S6 kinase 1 variant reveals a novel mammalian target of rapamycin phosphorylation site. J Biol Chem 277:20104–20112.

Sancak Y, Thoreen CC, Peterson TR, Lindquist RA, Kang SA, Spooner E, Carr SA, Sabatini DM. 2007. PRAS40 is an insulin-regulated inhibitor of the mTORC1 protein kinase. Mol Cell 25:903–915.

Sancak Y, Peterson TR, Shaul YD, Lindquist RA, Thoreen CC, Bar-Peled L, Sabatini DM. 2008. The Rag GTPases bind raptor and mediate amino acid signaling to mTORC1. Science 320:1496–1501.

Sarbassov DD, Ali SM, Kim DH, Guertin DA, Latek RR, Erdjument-Bromage H, Tempst P, Sabatini DM. 2004. Rictor, a novel binding partner of mTOR, defines a rapamycin-insensitive and raptor-independent pathway that regulates the cytoskeleton. Curr Biol 14:1296–1302.

Shaw RJ. 2009. LKB1 and AMP-activated protein kinase control of mTOR signalling and growth. Acta Physiol (Oxf) 196:65–80.

Shaw RJ, Cantley LC. 2006. Ras, PI(3)K and mTOR signalling controls tumour cell growth. Nature 441:424–430.

Soulsby MD, Alzayady K, Xu Q, Wojcikiewicz RJ. 2004. The contribution of serine residues 1588 and 1755 to phosphorylation of the type I inositol 1,4,5-trisphosphate receptor by PKA and PKG. FEBS Lett 557:181–184.

Tang TS, Tu H, Wang Z, Bezprozvanny I. 2003. Modulation of type 1 inositol (1,4,5)-trisphosphate receptor function by protein kinase a and protein phosphatase 1alpha. J Neurosci 23:403–415.

Tsang CK, Qi H, Liu LF, Zheng XF. 2007. Targeting mammalian target of rapamycin (mTOR) for health and diseases. Drug Discov Today 12:112–124.

Tu H, Tang TS, Wang Z, Bezprozvanny I. 2004. Association of type 1 inositol 1,4,5-trisphosphate receptor with AKAP9 (Yotiao) and protein kinase A. J Biol Chem 279:19375–19382.

Wagner LE II, Li WH, Joseph SK, Yule DI. 2004. Functional consequences of phosphomimetic mutations at key cAMP-dependent protein kinase phosphorylation sites in the type 1 inositol 1,4,5-trisphosphate receptor. J Biol Chem 279:46242–46252.

Wang CY, Kim HH, Hiroi Y, Sawada N, Salomone S, Benjamin LE, Walsh K, Moskowitz MA, Liao JK. 2009. Obesity increases vascular senescence and susceptibility to ischemic injury through chronic activation of Akt and mTOR. Sci Signal 2:ra11.

Wojcikiewicz RJ, He Y. 1995. Type I, II and III inositol 1,4,5-trisphosphate receptor co-immunoprecipitation as evidence for the existence of heterotetrameric receptor complexes. Biochem Biophys Res Commun 213: 334–341.

Yoshida Y, Imai S. 1997. Structure and function of inositol 1,4,5-trisphosphate receptor. Jpn J Pharmacol 74:125–137.